Int J Clin Exp Med 2017;10(5):8110-8117
www.ijcem.com /ISSN:1940-5901/IJCEM0050979

Original Article

Relationship of shear wave elastography findings with pathology in papillary thyroid carcinomas model

Jiying Gu[1], Huiping Zhang[1], Fan Li[1], Feng Gao[1], Yang Liu[1], Lingxi Xing[1], Lifang Jin[1], Xuemei Zhang[2], Lin Yuan[2], Lianfang Du[1]

Departments of [1]Ultrasound, [2]Pathology, Shanghai General Hospital, School of Medicine, Shanghai Jiao Tong University, Shanghai, China

Received February 16, 2017; Accepted March 17, 2017; Epub May 15, 2017; Published May 30, 2017

Abstract: We explored the relationship between shear wave elastography (SWE) findings and papillary thyroid carcinoma (PTC) pathology. BCPAP cells were subcutaneously injected into the thighs of nude mice. The resulting lesions were divided into two groups according to tumor size: diameter 5-10 mm, papillary thyroid microcarcinoma (PTMC) group; diameter 11-15 mm, PTC group. All tumors were examined using SWE. Platelet-derived growth factor (PDGF), vascular endothelial growth factor (VEGF), and microvessel density (MVD) were assessed immunohistochemically. The elastic values (E_{mean} and E_{max}) on SWE were significantly higher in the PTC group (26.695 ± 5.986 and 41.338 ± 9.643 kPa, respectively) than those in the PTMC group (16.842 ± 5.317 and 23.989 ± 6.315 kPa, respectively; $P < 0.05$). The PDGF expression and MVD were significantly higher in PTCs than those in PTMCs ($P < 0.05$). The elastic values were positively correlated with PDGF and MVD ($P < 0.05$). Maximum tumor diameter was positively correlated with elastic parameters, PDGF, and MVD ($P < 0.05$). We concluded that tumor stiffness was correlated with PDGF and MVD in PTCs and PDGF might play an important role in PTC development.

Keywords: Shear wave elastography, platelet-derived growth factor, vascular endothelial growth factor, microvessel density

Introduction

Papillary thyroid carcinoma (PTC) is the most common type of malignant thyroid tumor, accounting for 80%-90% of all thyroid malignancies [1]. Ultrasonography is the principal imaging method used for the detection of thyroid nodules. However, its diagnostic accuracy for papillary thyroid microcarcinomas (PTMCs) is low because of their small size (< 10 mm by definition) and atypical sonographic appearance; moreover, the technique is highly operator dependent [2, 3]. Shear wave elastography (SWE) is a new ultrasound technology in which shear waves are used to determine the hardness or stiffness of tissues. SWE can be used for the qualitative and quantitative assessment of focal lesions. During SWE, tissues are mechanically excited by acoustic radiation force impulses to generate small (1-10 mm), localized tissue displacements. The displacements result in shear wave propagation, which is tracked to calculate the shear wave velocity (SWV) or compute the Young modulus (E). The method works from the assumption that most malignancies are composed of "hard/stiff" tissue and that benign tumors are composed of "soft" tissue [4, 5].

Tumor stiffness has been shown to predict invasive potential as well as response to therapy in a number of cancers such as breast cancer, hepatocellular carcinoma, and meningioma [6-9]. Thus, tumor stiffness may be useful to differentiate malignant from benign lesions and predict prognosis, metastatic potential, and treatment outcomes [10, 11]. Additionally, the identification of the molecular pathological factors determining tumor stiffness may provide novel therapeutic targets in various cancers. However, the pathological basis for the difference in tissue stiffness between benign and malignant thyroid tumors remains unknown. Several factors are responsible for the hardness/stiffness of tumor tissues, including angiogenesis and fibrosis [12, 13]. Microvessel

density (MVD) is a measure of tumor angiogenesis [14]. Vascular endothelial growth factor (VEGF) is a well-known angiogenetic factor that has been shown to contribute to the progression of several tumors, such as renal cell carcinoma, prostate cancer, breast cancer, and thyroid carcinoma [15-19]. Platelet-derived growth factor (PDGF) has been associated with angiogenesis and myofibroblast proliferation in fibrosis [20, 21].

The purpose of this study was to quantitatively assess the stiffness of thyroid tumors in nude mice by using SWE and to correlate the results with histopathological features such as MVD, and VEGF and PDGF expression to deepen our understanding of the pathological processes determining tumor stiffness and identify potential tumor markers and therapeutic targets.

Materials and methods

Animals

This study was performed on 12 male BALB/C nude mice aged 4-6 weeks. The PTC cell line BCPAP was subcutaneously injected into the right thighs of the mice (3×10^7 cells/mouse). Tumor growth was closely monitored until the tumor diameter exceeded 5 mm (which took approximately 19-22 days); the mice were then divided into two groups: PTMC group (maximum tumor diameter 5-10 mm) and PTC group (maximum tumor diameter 11-15 mm). The mice were then subjected to SWE and subsequently sacrificed by cervical dislocation. All tumors were excised, measured, and fixed for immunohistochemical staining. The animal experimental protocol was approved by the ethics committee of Shanghai General Hospital Affiliated TO Shanghai Jiao Tong University and was performed in accordance with ethical principles. The mice were handled and housed according to protocols approved by the Shanghai Medical Experimental Animal Care Commission.

Cell culture and reagents

BCPAP cells, which are characterized by the *BRAF* V600E mutation, were generously provided by Dr. Ma Chao (Xinhua Hospital affiliated to Shanghai Jiao Tong University, China). The cells were grown in a mixture of MCDB 105 (Sigma-Aldrich Trading Co. Ltd., Shanghai, China) and DMEM-F12 supplemented with 10% fetal bovine serum (Sigma) in a humidified atmosphere containing 5% CO_2 at 37°C for 3-5 days. A mouse monoclonal anti-human CD34 antibody and a broad-spectrum secondary antibody were purchased from Abcam (Cambridge, UK). Purified rabbit polyclonal anti-human VEGFR2 antibody and anti-PDGFR-β antibody were purchased from Abcam (Cambridge, UK).

SWE

All tumors were assessed using the Aixplorer ultrasound scanner (Supersonic Imagine, Aix en Provence, France), which was equipped with a 4-15 MHz linear transducer. Nude mice were anesthetized and fixed in a supine position, and the lesion and surrounding thigh area were exposed. After performing an ultrasound examination, the transducer was switched to the SWE mode. The lesion and surrounding tissues were defined as the region of interest. To obtain appropriate images, the probe was applied as lightly as possible in order to minimize compression artifacts, and the appropriate ultrasound coupling agents were used to ensure complete contact with the lesions. It is worth noting that the probe must be kept stably during the examination. The elastographic findings were displayed in different colors, with red representing harder tissues, and blue indicating softer tissues. After a stable image had been recorded, a Q-box (diameter, 2 mm) that covered the hardest part of the lesion was selected to calculate the elasticity value. The Young modulus (E_{mean}, E_{min}, and E_{max}) in the Q-box was calculated. Three Q-boxes were placed over each lesion, and the average value was used in the final analysis.

Immunohistochemical analysis

The presence of CD34, VEGF, and PDGF were analyzed using immunohistochemistry with the Envision detection system (Dako) according to standard procedures. Thyroid specimens were fixed with 10% formaldehyde, embedded in paraffin, sliced into 4-μm sections, and baked at 60°C overnight. The sections were rinsed three times in phosphate-buffered solution (PBS; 0.01 mol/L, pH 7.4) and incubated in hydrogen peroxide in methanol for 30 min. The sections were then incubated overnight with rabbit anti-human polyclonal VEGFR2 antibody (1:50), mouse anti-human monoclonal CD34 antibody (1:100), and rabbit anti-human PDGF-β poly-

Table 1. SWE findings, PDGF expression, and angiogenesis in PTC and PTMC

	PTMC	PTC	Average	Z and *p* values
Number of mice	6	6	/	/
Duration of tumor growth (days)	19	22	/	/
Maximum tumor diameter (mm)	8.283 ± 1.010	12.283 ± 1.401	10.050 ± 2.065	P = 0.001
E_{mean} (kPa)	16.842 ± 5.317	26.695 ± 5.986	21.769 ± 7.458	-2.402, 0.015
E_{min} (kPa)	11.579 ± 6.370	13.889 ± 3.944	12.734 ± 5.193	-0.642, 0.589
E_{max} (kPa)	23.989 ± 6.315	41.338 ± 9.643	32.663 ± 11.937	-2.722, 0.004
PDGF	2.347 ± 0.436	2.946 ± 0.255	2.647 ± 0.462	-2.402, 0.015
MVD	24.933 ± 3.058	32.950 ± 9.483	28.942 ± 7.916	-2.246, 0.026
VEGF expression	(+), 2 tumors; (++), 2 tumors; (+++), 2 tumors	(+), 1 tumor; (++), 5 tumors	/	-0.361, 0.818

E, Young modulus; MVD, microvessel density; PDGF, platelet-derived growth factor; PTC, papillary thyroid carcinoma; PTMC, papillary thyroid microcarcinoma; SWE, shear wave elastography; VEGF, vascular endothelial growth factor. Values are shown as mean ± standard deviation or absolute numbers. VEGF expression: (+), weakly positive, < 25% positively stained cells; (++), moderately positive, 25%-50% positively stained cells; and (+++), strongly positive, > 50% positive cells.

clonal antibody (1:50) at 4°C, and again washed three times in PBS. Next, the sections were incubated with Envision polymer (Dako) for 60 min. Finally, the sections were counterstained with hematoxylin, dehydrated, and mounted in resinous mountant. Negative controls with PBS (0.01 mol/L, pH 7.4) replacing the primary antibody were also included.

Microvessels labeled with the CD34 antibody were counted using the Weidner procedure [22]. Five random areas with the highest MVD were selected under low magnification (× 100), and the microvessels were counted under high magnification (× 400). Vascular endothelial cells or cell clusters in the intercellular substance that stained brown were considered positive. The average MVD of the five areas was considered as the MVD of the tumor.

VEGF immunoreactivity was assessed using a semi-quantitative method [23]. Five areas were randomly selected under high magnification, and the percentage of brown-stained tumor cells in these areas was graded as follows: negative (-), no positively stained cells in the entire slice; weakly positive (+), < 25% positively stained cells; moderately positive (++), 25%-50% cells; and strongly positive (+++), > 50% positive cells. Lesions with no or slightly positive staining were considered to have low VEGF expression, while lesions with moderately or strongly positive staining were considered to have high VEGF expression. Both MVD and VEGF expression were separately evaluated by two pathologists.

PDGF expression was assessed using H-scores [24]. Ten areas were randomly selected under low magnification (× 10), and in each area, 50 cells were randomly counted under high magnification (× 400). The intensity of staining was categorized as follows: 0, negative; 1, weak (light yellow); 2, moderate (yellow-brown); and 3, strong (brown). The H-score, which fully reflects the PDGFRβ expression in the tumor cells, was calculated according to the following formula: H-score = Σ (i + 1) Pi where i is the staining intensity (1, 2, or 3), and Pi = the number of cells scored as i/total number of cells in all 10 areas × 100%).

Statistical analysis

Statistical analysis was performed using SPSS 13.0 software. All measurement data were presented as mean ± SD. SWE, PDGF, VEGF, and MVD data were compared using the Mann-Whitney *U*-test, while correlations were assessed using the Pearson test. The level of significance was set at $P < 0.05$ (Fisher exact test).

Results

Ultrasound and SWE

In all 12 mice, the thyroid lesions appeared uniformly hypoechoic with a well-defined boundary, without calcifications or liquefaction. The lesion size ranged from 3.2 × 7.8 mm to 8.0 × 13.8 mm. The average vertical diameter was 5.867 ± 1.703 mm, and the average maximum diameter was 10.050 ± 2.065 mm. According to the tumor size, six mice were assigned to the PTC group, and six were assigned to the PTMC group. The maximum tumor diameter was 8.283 ± 1.010 mm in the PTMC group and 12.283 ± 1.401 mm in the PTC group ($P < 0.05$).

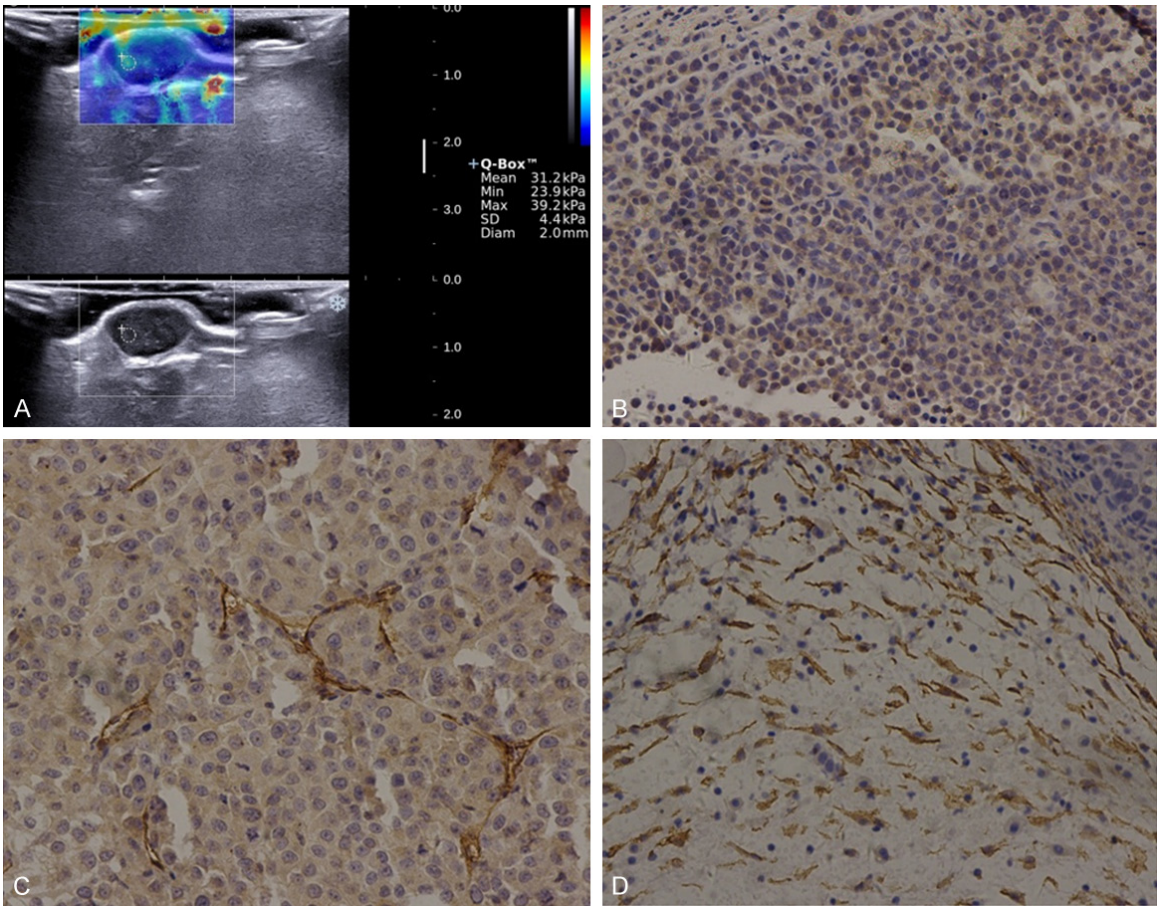

Figure 1. Papillary thyroid carcinoma. A. Shear wave elastography. Tumor size, 7.8 mm × 13.3 mm; E_{mean}, 31.2 kPa; E_{min}, 23.9 kPa; E_{max}, 39.2 kPa. B. The lesion is strongly positive for VEGF expression (+++; × 200). C. The average number of microvessels was 35 vessels/field according to the EnVision technique (× 400). D. PDGF expression was scored as 3.16 (× 200).

The average elastic parameters of the thyroid nodules were as follows: E_{mean} = 21.769 ± 7.458 kPa; E_{min} = 12.734 ± 5.193 kPa, and E_{max} = 32.663 ± 11.937 kPa (**Table 1**). All elastic parameters were higher in the PTC group than in the PTMC (**Figures 1A** and **2A**), with the difference being statistically significant for E_{mean} and E_{max} ($P < 0.05$). E_{mean} and E_{max} were positively correlated with the maximum tumor diameter ($P < 0.05$; **Table 2**).

VEGF expression and MVD

VEGF expression was positive in all tumors: three tumors were slightly positive (**Figure 2B**), seven were moderately positive, and two were strongly positive for VEGF expression (**Figure 1B**). The difference in VEGF expression between the two groups was not statistically significant ($Z = -0.361$, $P = 0.818$; **Table 1**).

All thyroid specimens were positively stained with the CD34 antibody. MVD was significantly higher in the PTC group (32.950 ± 9.483 vessels/field) than in the PTMC group (24.933 ± 3.058 vessels/field, $Z = -2.246$, $P = 0.026$; **Figures 1C** and **2C**; **Table 1**). MVD was positively correlated with maximum tumor diameter ($P < 0.05$; **Table 2**).

PDGF expression

The average PDGF expression score in all lesions was 2.647 ± 0.462. The score in the PTC group (2.946 ± 0.255) was significantly higher than that in the PTMC group (2.347 ± 0.436, $Z = -2.402$, $p = 0.015$; **Figures 1D** and **2D**; **Table 1**). PDGF expression was positively correlated with maximum tumor diameter ($P < 0.05$; **Table 2**).

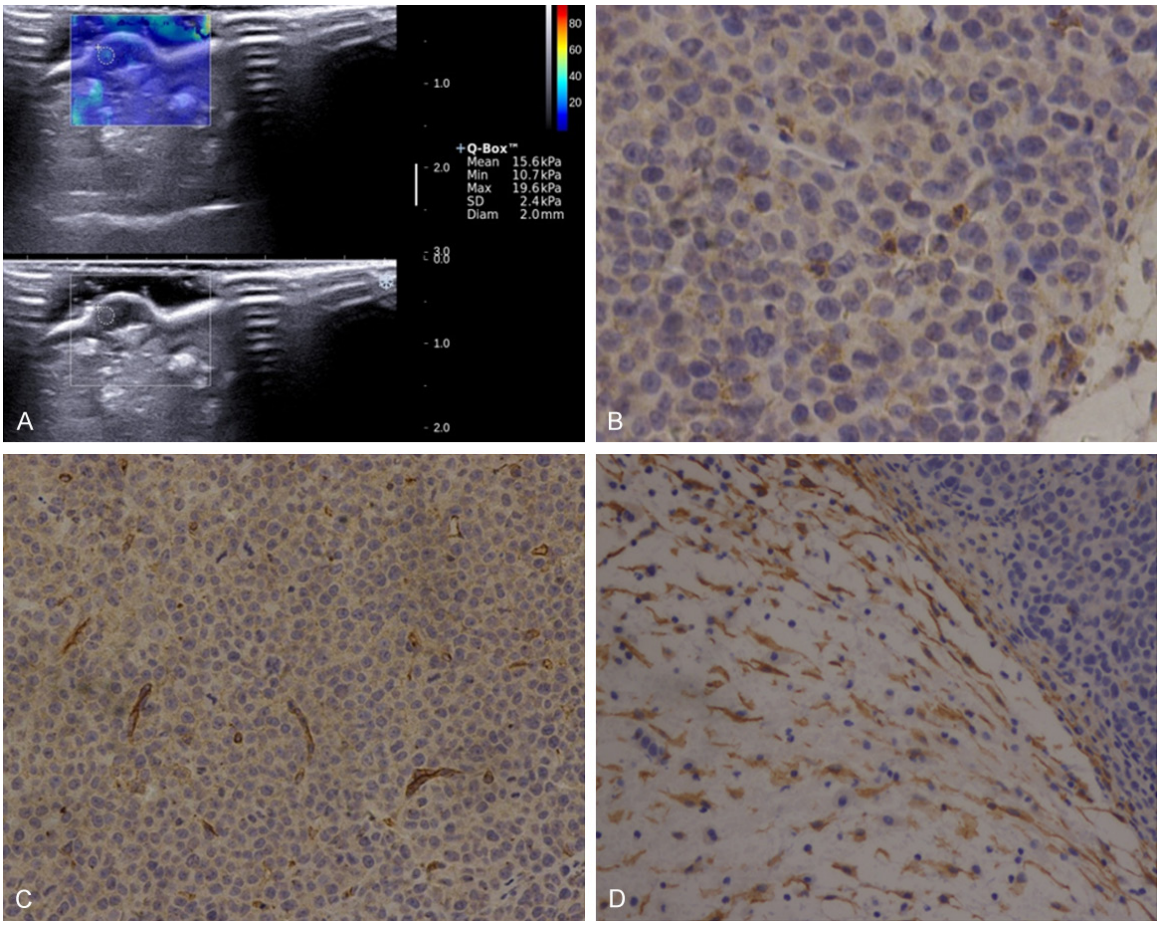

Figure 2. Papillary thyroid microcarcinoma. A. Shear wave elastography. Tumor size, 3.5 mm × 8.6 mm; E_{mean}, 15.6 kPa; E_{min}, 10.7 kPa; E_{max}, 19.6 kPa. B. The lesion is weakly positive for VEGF expression (+; × 200). C. The average number of microvessels was 24 vessels/field according to the EnVision technique (× 200). D. PDGF expression was scored as 2.15 (× 200).

Table 2. Correlation of maximum tumor diameter with elastic parameters, PDGF, and angiogenesis

	E_{mean} (r, p)	E_{min} (r, p)	E_{max} (r, p)	Maximum tumor diameter
Maximum tumor diameter	0.776, 0.003	0.326, 0.301	0.797, 0.002	/
PDGF	0.787, 0.002	0.641, 0.025	0.617, 0.033	0.748, 0.005
MVD	0.604, 0.038	0.214, 0.504	0.694, 0.012	0.715, 0.009
VEGF	0.226, 0.479	0.610, 0.035	0.118, 0.714	0.146, 0.651

E, Young modulus; MVD, microvessel density; PDGF, platelet-derived growth factor; VEGF, vascular endothelial growth factor.

Correlations between PDGF, angiogenesis, and elasticity

E_{mean}, E_{min}, and E_{max} were positively correlated with PDGF ($P < 0.05$; **Table 2**); E_{mean} and E_{max} were positively correlated with MVD ($P < 0.05$); and PDGF was slightly correlated with MVD ($r = 0.577$, $P = 0.049$). PDGF expression, MVD, and elastic stiffness gradually increased with tumor size. VEGF was not correlated with elastic parameters ($P > 0.05$), PDGF ($r = -0.108$, $P = 0.739$) or MVD ($r = 0.09$, $P = 0.781$).

Discussion

This study found that tissue hardness, MVD, and PDGF expression were correlated with tumor size. All three parameters were significantly higher in the PTC group than in the PTMC group. MVD was positively correlated with elas-

tic parameters (E_{mean} and E_{max}) and slightly correlated with PDGF. However, VEGF was not correlated with MVD, PDGF, or elastic parameters. These findings indicate that PDGF may play an important role in the development of tumor stiffness and angiogenesis in PTC.

Studies have shown that SWE can be used to differentiate the malignant from benign thyroid nodules [25, 26]. Varying SWVs have been reported for malignant nodules. Park *et al.* reported the following the cutoff values for predicting malignancy were: E_{mean}, 85.2 kPa; E_{max}, 94.0 kPa; and E_{min}, 54.0 kPa [27]. Samir *et al.* reported that the mean Young modulus estimate for malignant thyroid nodules was 31.69 kPa (10.97-50.31 kPa), and recommended a cutoff value of 22.30 kPa for diagnosing thyroid malignancy [28]. In our study, tumor stiffness was higher in the PTC group than in the PTMC group, which is consistent with the report that tumor stiffness increases with the size and growth of breast cancers [29]. However, the elastic parameters calculated in our study were lower than those previously reported. This difference is likely attributable to the following reasons: (1) Our study was conducted in nude mice, which show rapid tumor growth as compared to human tumors; this may partially account for the lower tumor stiffness in this experiment. (2) None of the tumors in our study had calcifications or inflammation, which are known to increase tissue stiffness [30]. (3) Finally, the tumor lesions in our study protruded from the thigh surface, and the impact force exerted by the probe may have been uneven, resulting in lower elastic parameters.

MVD in PTC has been reported to vary from 26.7 to 103.6 vessels/field [31-33]. This variation in MVD values is likely attributable to the differences in measurement techniques (e.g., the use of different vascular markers and different methods of counting microvessels) as well as interindividual differences and differences in pathological tumor stages. However, regardless of the assessment method, MVD has been found to be higher in PTCs than in other thyroid nodules (e.g., thyroid follicular carcinoma and adenoma), and patients with higher MVD have a worse prognosis than those with lower MVD [34, 35]. In our study, MVD was 24.933 ± 3.058 vessels/field in the PTMC group and 32.950 ± 9.483 vessels/field in the PTC group, which indicates that invasive potential and microvessel quantity increased with tumor growth. This explains why anti-angiogenic drugs inhibit tumor growth and metastasis.

VEGF has been significantly correlated with angiogenesis, lymph node metastasis, and distant metastasis in PTC [17, 18]. However, in our study, VEGF expression was not correlated with MVD probably because the tumors were in the early stages, the mouse survival duration was short, and there were no metastases. Gulubova *et al*. [34] also reported that VEGF expression is not correlated with MVD in any thyroid cancer types.

PDGF is a potent mitogen and chemotactic factor for a variety of mesenchymal cells, such as fibroblasts and vascular smooth muscle cells. PDGF plays a major role in the replication, survival, and migration of myofibroblasts during the pathogenesis of fibrotic diseases [20, 21]. Breast cancer cells can produce PDGF-BB, and its receptor can stimulate fibroblast growth [36]. Our study found that PDGF expression is higher in PTC than in PTMC, and is positively correlated with elastic parameters. PDGF expression and fibrosis increased with tumor size and growth, leading to harder tumors. Thus, PDGF expression reflects PTC stiffness.

Our study has some limitations. First, the sample size was small. Only two experimental groups could be formed according to tumor size because of rapid tumor growth. Second, we assessed only PTCs because they are the most common thyroid tumors. Further large-scale investigations are necessary to determine the cause of the increased stiffness in PTCs and to explore the role of the microenvironment in thyroid carcinoma.

We found that tumor stiffness was correlated with tumor size; thus, SWE may be useful to differentiate malignant from benign thyroid nodules. Additionally, MVD and PDGF expression were correlated with tumor stiffness and increased with tumor growth. Thus, PDGF may be involved in thyroid tumor progression and may be a novel therapeutic target in PTC. The findings indicate a rationale for the potential use of anti-angiogenic and anti-fibrotic treatments in PTC.

Acknowledgements

We are grateful for the support of Laboratory Center of Shanghai General Hospital. This work was supported by the National Natural Science

Foundation (grant number: 81301232, 8120-1100, 81401415), Shanghai Municipal Health Bureau (grant number: 20124205).

Disclosure of conflict of interest

None.

Address correspondence to: Lianfang Du, Department of Medical Ultrasound, Shanghai General Hospital, School of Medicine, Shanghai Jiao Tong University, 100 Haining Road, Shanghai 200080, China. Tel: +8613386259562; E-mail: du_lf@163.com

References

[1] Wiltshire JJ, Drake TM, Uttley L, Balasubramanian SP. Systematic review of trends in the incidence rates of thyroid cancer. Thyroid 2016; 26: 1541-1552.

[2] Moon HJ, Sung JM, Kim EK, Yoon JH, Youk JH, Kwak JY. Diagnostic performance of gray-scale US and elastography in solid thyroid nodules. Radiology 2012; 262: 1002-1013.

[3] Unluturk U, Erdogan MF, Demir O, Gullu S, Baskal N. Ultrasound elastography is not superior to grayscale ultrasound in predicting malignancy in thyroid nodules. Thyroid 2012; 22: 1031-1038.

[4] Bhatia KS, Tong CS, Cho CC, Yuen EH, Lee YY, Ahuja AT. Shear wave elastography of thyroid nodules in routine clinical practice: preliminary observations and utility for detecting malignancy. Eur Radiol 2012; 22: 2397-2406.

[5] Dudea SM, Botar-Jid C. Ultrasound elastography in thyroid disease. Med Ultrason 2015; 17: 74-96.

[6] Hayashi M, Yamamoto Y, Ibusuki M, Fujiwara S, Yamamoto S, Tomita S, Nakano M, Murakami K, Iyama K, Iwase H. Evaluation of tumor stiffness by elastography is predictive for pathologic complete response to neoadjuvant chemotherapy in patients with breast cancer. Ann Surg Oncol 2012; 19: 3042-3049.

[7] Cho SH, Lee JY, Han JK, Choi BI. Acoustic radiation force impulse elastography for the evaluation of focal solid hepatic lesions: preliminary findings. Ultrasound Med Biol 2010; 36: 202-208.

[8] Murphy MC, Huston J 3rd, Glaser KJ, Manduca A, Meyer FB, Lanzino G, Morris JM, Felmlee JP, Ehman RL. Preoperative assessment of meningioma stiffness using magnetic resonance elastography. J Neurosurg 2013; 118: 643-648.

[9] Kwon HJ, Kang MJ, Cho JH, Oh JY, Nam KJ, Han SY, Lee SW. Acoustic radiation force impulse elastography for hepatocellular carcinoma-associated radiofrequency ablation. World J Gastroenterol 2011; 17: 1874-1878.

[10] Evans A, Whelehan P, Thomson K, McLean D, Brauer K, Purdie C, Baker L, Jordan L, Rauchhaus P, Thompson A. Invasive breast cancer: relationship between shear-wave elastographic findings and histologic prognostic factors. Radiology 2012; 263: 673-677.

[11] Swaminathan V, Mythreye K, O'Brien ET, Berchuck A, Blobe GC, Superfine R. Mechanical stiffness grades metastatic potential in patient tumor cells and in cancer cell lines. Cancer Res 2011; 71: 5075-5080.

[12] Sieminski AL, Hebbel RP, Gooch KJ. The relative magnitudes of endothelial force generation and matrix stiffness modulate capillary morphogenesis in vitro. Exp Cell Res 2004; 297: 574-584.

[13] Masuzaki R, Tateishi R, Yoshida H, Sato T, Ohki T, Goto T, Yoshida H, Sato S, Sugioka Y, Ikeda H, Shiina S, Kawabe T, Omata M. Assessing liver tumor stiffness by transient elastography. Hepatol Int 2007; 1: 394-397.

[14] de la Torre NG, Buley I, Wass JA, Turner HE. Angiogenesis and lymphangiogenesis in thyroid proliferative lesions: relationship to type and tumour behaviour. Endocr Relat Cancer 2006; 13: 931-944.

[15] Muhl L, Moessinger C, Adzemovic MZ, Dijkstra MH, Nilsson I, Zeitelhofer M, Hagberg CE, Huusko J, Falkevall A, Yla-Herttuala S, Eriksson U. Expression of vascular endothelial growth factor (VEGF)-B and its receptor (VEGFR1) in murine heart, lung and kidney. Cell Tissue Res 2016; 365: 51-63.

[16] Liu ZQ, Fang JM, Xiao YY, Zhao Y, Cui R, Hu F, Xu Q. Prognostic role of vascular endothelial growth factor in prostate cancer: a systematic review and meta-analysis. Int J Clin Exp Med 2015; 8: 2289-2298.

[17] Karlikova M, Topolcan O, Narsanska A, Kucera R, Treskova I, Treska V. Circulating growth and angiogenic factors and lymph node status in early-stage breast cancer-a pilot study. Anticancer Res 2016; 36: 4209-4214.

[18] Byrne AM, Bouchier-Hayes DJ, Harmey JH. Angiogenic and cell survival functions of vascular endothelial growth factor (VEGF). J Cell Mol Med 2005; 9: 777-794.

[19] Yasuoka H, Nakamura Y, Zuo H, Tang W, Takamura Y, Miyauchi A, Nakamura M, Mori I, Kakudo K. VEGF-D expression and lymph vessels play an important role for lymph node metastasis in papillary thyroid carcinoma. Mod Pathol 2005; 18: 1127-1133.

[20] Cumpănas AA, Cimpean AM, Ferician O, Ceausu RA, Sarb S, Barbos V, Dema A, Raica M. The involvement of PDGF-B/PDGFRβ axis in

the resistance to antiangiogenic and antivascular therapy in renal cancer. Anticancer Res 2016; 36: 2291-2295.
[21] Cheng X, Tsao C, Sylvia VL, Cornet D, Nicolella DP, Bredbenner TL, Christy RJ. Platelet-derived growth-factor-releasing aligned collagen-nanoparticle fibers promote the proliferation and tenogenic differentiation of adipose-derived stem cells. Acta Biomater 2014; 10: 1360-1369.
[22] Weidner N. Current pathologic methods for measuring intratumoral microvessel density within breast carcinoma and other solid tumors. Breast Cancer Res Treat 1995; 36: 169-180.
[23] Volm M, Koomagi R, Mattern J. Prognostic value of vascular endothelial growth factor and its receptor Flt-1 in squamous cell lung cancer. Int J Cancer 1997; 74: 64-68.
[24] Harrington DJ, Lessey BA, Rai V, Bergqvist A, Kennedy S, Manek S, Barlow DH, Mardon HJ. Tenascin is differentially expressed in endometrium and endometriosis. J Pathol 1999; 187: 242-248.
[25] Lin P, Chen M, Liu B, Wang S, Li X. Diagnostic performance of shear wave elastography in the identification of malignant thyroid nodules: a meta-analysis. Eur Radiol 2014; 24: 2729-2738.
[26] Fukuhara T, Matsuda E, Fujiwara K, Tanimura C, Izawa S, Kataoka H, Kitano H. Phantom experiment and clinical utility of quantitative shear wave elastography for differentiating thyroid nodules. Endocr J 2014; 61: 615-621.
[27] Park AY, Son EJ, Han K, Youk JH, Kim JA, Park CS. Shear wave elastography of thyroid nodules for the prediction of malignancy in a large scale study. Eur J Radiol 2015; 84: 407-412.
[28] Samir AE, Dhyani M, Anvari A, Prescott J, Halpern EF, Faquin WC, Stephen A. Shear-wave elastography for the preoperative risk stratification of follicular-patterned lesions of the thyroid: diagnostic accuracy and optimal measurement plane. Radiology 2015; 277: 565-573.
[29] Chamming's F, Latorre-Ossa H, Le Frere-Belda MA, Fitoussi V, Quibel T, Assayag F, Marangoni E, Autret G, Balvay D, Pidial L, Gennisson JL, Tanter M, Cuenod CA, Clement O, Fournier LS. Shear wave elastography of tumour growth in a human breast cancer model with pathological correlation. Eur Radiol 2013; 23: 2079-2086.
[30] Szczepanek-Parulska E, Wolinski K, Stangierski A, Gurgul E, Ruchala M. Biochemical and ultrasonographic parameters influencing thyroid nodules elasticity. Endocrine 2014; 47: 519-527.
[31] Lee SH, Lee SJ, Jin SM, Lee NH, Kim DH, Chae SW, Sohn JH, Kim WS. Relationships between lymph node metastasis and expression of CD31, D2-40, and vascular endothelial growth factors a and c in papillary thyroid cancer. Clin Exp Otorhinolaryngol 2012; 5: 150-155.
[32] Wei X, Li Y, Zhang S, Ming G. Evaluation of thyroid cancer in Chinese females with breast cancer by vascular endothelial growth factor (VEGF), microvessel density, and contrast-enhanced ultrasound (CEUS). Tumour Biol 2014; 35: 6521-6529.
[33] Zhou Q, Jiang J, Shang X, Zhang HL, Ma WQ, Xu YB, Wang H, Li M. Correlation of contrast-enhanced ultrasonographic features with microvessel density in papillary thyroid carcinomas. Asian Pac J Cancer Prev 2014; 15: 7449-7452.
[34] Gulubova M, Ivanova K, Ananiev J, Gerenova J, Zdraveski A, Stoyanov H, Vlaykova T. VEGF expression, microvessel density and dendritic cell decrease in thyroid cancer. Biotechnol Biotechnol Equip 2014; 28: 508-517.
[35] Jebreel A, England J, Bedford K, Murphy J, Karsai L, Atkin S. Vascular endothelial growth factor (VEGF), VEGF receptors expression and microvascular density in benign and malignant thyroid diseases. Int J Exp Pathol 2007; 88: 271-277.
[36] Gehmert S, Gehmert S, Prantl L, Vykoukal J, Alt E, Song YH. Breast cancer cells attract the migration of adipose tissue-derived stem cells via the PDGF-BB/PDGFR-beta signaling pathway. Biochem Biophys Res Commun 2010; 398: 601-605.